BBA - General Subjects 1864 (2020) 129450

Contents lists available at ScienceDirect

BBA - General Subjects

journal homepage: www.elsevier.com/locate/bbagen

Spatial arrangement of LD motif-interacting residues on focal adhesion targeting domain of Focal Adhesion Kinase determine domain-motif interaction affinity and specificity

Anjali Bansal Gupta[a], Somsubhro Mukherjee[a,b], Catherine Quirong Pan[a], Adrian Velazquez-Campoy[d,e,f,g,h], J. Sivaraman[b], Boon Chuan Low[a,b,c,*]

[a] Mechanobiology Institute, National University of Singapore, Republic of Singapore
[b] Department of Biological Sciences, National University of Singapore, Republic of Singapore
[c] University Scholars Programme, National University of Singapore, Republic of Singapore
[d] Institute of Biocomputation and Physics of Complex Systems (BIFI), Joint Units IQFR-CSIC-BIFI, GBsC-CSIC-BIFI, Universidad de Zaragoza, Zaragoza, Spain
[e] Department of Biochemistry and Molecular and Cell Biology, Universidad de Zaragoza, Zaragoza, Spain
[f] Aragon Institute for Health Research (IIS Aragon), Zaragoza, Spain
[g] Biomedical Research Networking Centre for Liver and Digestive Diseases (CIBERehd), Madrid, Spain
[h] Fundacion ARAID, Government of Aragon, Zaragoza, Spain

ARTICLE INFO

Keywords:
LD motif
Focal adhesion
Protein-protein interaction
Isothermal titration calorimetry (ITC)
Protein domain
Protein purification

ABSTRACT

Background: Leucine rich Aspartate motifs (LD motifs) are molecular recognition motifs on Paxillin that recognize LD-motif binding domains (LDBD) of a number of focal adhesion proteins in order to carry out downstream signaling and actin cytoskeleton remodeling. In this study, we identified structural features within LDBDs that influence their binding affinity with Paxillin LD motifs.

Methods: Various point mutants of focal adhesion targeting (FAT) domain of Focal Adhesion Kinase (FAK) were created by moving a key Lysine residue two and three helical turns in order to match the unique conformations as observed in LDBDs of two other focal adhesion proteins, Vinculin and CCM3.

Results: This led to identify a mutant of FAT domain of FAK, named as FAT(NV) (Asn992 of FAT domain was replaced by Val), with remarkable high affinity for LD1 (K_d = 1.5 μM vs no-binding with wild type) and LD2 peptides (K_d = 7.2 μM vs 63 μM with wild type). Consistently, the focal adhesions of MCF7 cells expressing FAK (NV) were highly stable (turnover rate = 1.25×10^{-5} μm^2/s) as compared to wild type FAK transfected cells (turnover rate = 1.5×10^{-3} μm^2/s).

Conclusions: We observed that the relative disposition of key LD binding amino-acids at LDBD surface, hydrophobic burial of long Leucine side chains of LD-motifs and complementarity of charged surfaces are the key factors determining the binding affinities of LD motifs with LDBDs.

General significance: Our study will help in protein engineering of FAT domain of FAK by modulating FAK-LD motif interactions which have implications in cellular focal adhesions and cell migration.

1. Introduction

Paxillin is a 68 kDa scaffold protein with four LIM domains at its C-terminus [1,2]. The N-terminus of Paxillin is highly disordered and contains structural motifs rich in Leucine and starting with Leucine and Aspartate residues, hence named Leucine rich Aspartate motifs (LD motifs) [3,4]. The LD motifs have a conserved sequence motif LDxLLxxL that folds as an amphipathic alpha helix [3]. Five LD motifs are present at Paxillin N-terminus and they are named from LD1 to LD5 in the order they are located on Paxillin sequence. While the knowledge on binding partners for LD3 and LD5 motifs is limited [5,6], other LD motifs (LD1, LD2, LD4) play an important role in focal adhesion biology as many of the structural and signaling molecules are localized to focal adhesions (FAs) through interaction with LD motifs [3,7]. Moreover, they compete with other similar LD-like motifs and thus regulate cell migration [8].

Abbreviations: ITC, Isothermal titration calorimetry; FAT domain, Focal adhesion targeting domain; FAK, Focal Adhesion Kinase; LD motifs, Leucine rich Aspartate motifs; LDBD, LD-motif binding domains; CCM3, Cerebral Cavernous Malformations 3

* Corresponding author at: Mechanobiology Institute, National University of Singapore, Republic of Singapore.
E-mail address: dbslowbc@nus.edu.sg (B.C. Low).

https://doi.org/10.1016/j.bbagen.2019.129450
Received 8 May 2019; Received in revised form 22 August 2019; Accepted 18 September 2019
Available online 30 October 2019

Sequences similar to LD motifs have been identified in several other proteins [4,9] however their function and binding partners remain unknown. Recently, LD-like motifs were identified in Cerebral Cavernous Malformations (CCM2) [10], Rho GTPase activating protein called Deleted in Liver Cancer1 (DLC1) [11] and in an intrinsically disordered translocated actin recruiting phosphoprotein (TarP) of Chlamydia [12]. The LD-like motif of CCM2 helps in mediating domain interaction with CCM3 to protect the proteins from proteasomal degradation [10]. Chlamydia TarP LD motif competes with mammalian Paxillin LD motif for interaction with Focal adhesion Kinase (FAK) leading to focal adhesion formation and thus cellular migration [12]. Similar competitive behavior is identified for the LD-like motif of DLC1, a tumor suppressor RhoGAP protein [11]. Similar to Paxillin LD motif, the DLC1 LD-like motif binds Talin and FAK and has been shown to be required for full tumor suppressor activity of DLC1 [11,13]. Thus, LD motifs are emerging as an important class of protein-protein interaction motifs implicated in host pathogen interactions, cancer metastasis, and brain disorders.

The protein domains that exhibit affinity for LD motifs (LD motif binding domains, LDBDs) have variable sequence and structural fold [14]. Most of them fold into a typical alpha-helical bundle [15], however there are exceptions from this trend such as α-parvin [16] and BPV E6 protein, which have two Zinc fingers [17]. LD motifs recognize a number of focal adhesion proteins, such as FAK [18], GIT [19], Pyk2 [20,21], Vinculin [22–24], β-parvin [25], Talin [13], Integrin [26], Kindlin-2 [27] and non-focal adhesion proteins such as CCM3 [7,28].

Same LD motif can bind to various LDBDs with varying affinities. For example, LD4 binds with high affinity to Focal adhesion targeting domain of Focal adhesion kinase (FAKFAT), but with low affinity to CCM3 [28]. Similarly, LD1 shows high affinity for CCM3 (K_d: 17 μM) [28], while it does not bind FAKFAT domain. LDBDs also bind selectively to certain LD motifs although the key interacting residues remain the same. For example, FAKFAT binds strongly with LD4 but does not interact with LD1. Various factors such as presence of conserved flanking residues near core LD motifs, variations within LD motifs, and length of LD motifs are suggested to influence the strength of LD-motif interaction with LDBDs. The variations in binding affinity range from no binding to as high as 1 μM [28]. In this study, we scrutinized the key elements critical for determining the binding affinity of LD motifs with LDBDs by analyzing available crystal structures, docking and isothermal titration calorimetry (ITC). Subsequently, the results were verified by cell-based experiments. We identify the hitherto unknown conformational requirement of key interacting amino acids and their relative positions.

2. Materials and methods

2.1. Sequence alignments and phylogenetic tree

Sequences of Paxillin, Hic5, PaxB and Leupaxin from *Dictyostellium*, *Drosophila*, *Gallus*, *Xenopus*, *Danio* and human were obtained from NCBI database and aligned by ClustalX v2.1 [29]. The LD motif sequences from Gelsolin, CCM2, DLC1, DLC2, RoXaN, Clamydia and others from the literature [4,10,12,14] were also added to the dataset. The phylogenetic tree was predicted using the neighbor-joining method [30], 1000 bootstrap trials and was displayed using iTOL online server [31].

2.2. Retrieving and analyzing three dimensional structures from Protein Data Bank

Three dimensional atomic coordinates of LD binding domains of FAKFAT (PDB ID: 1OW6, 1OW7, 1OW8) [32], CCM3 (PDB ID: 3RQE, 3RQF, 3RQG) [28], α-parvin (PDB ID: 2VZD, 2VZG, 2VZI) [16] in complex with LD1, LD2, and LD4 peptides were retrieved from RCSB Protein Data Bank (PDB) [33]. PDB file corresponding to Vinculin tail domain (PDB ID: 3H2U) [34] was also extracted, although it is not in complex with any LD motif. Supplementary Table S1 summarizes the structures obtained and analyzed for LD motif binding and those that bind to LD motifs.

'Contact' module available as part of CCP4 suite of programs was used to identify atomic contacts falling below a cut-off distance of 4 Å. No contacts of hydrogen atoms were included in the calculation. Hydrophobic interactions were estimated by counting the number of Cα atom pairs from two chains. Electrostatic interactions were the interactions between two electronegative atoms from two separate chains.

2.3. Molecular docking using HADDOCK

LD1, LD2 and LD4 peptides were extracted from α-parvin-LD complexes (from PDB IDs: 2VZD, 2VZG and 2VZI respectively) [16]. These were docked on LDBDs of FAK (PDB ID: 1OW6), CCM3 (PDB ID: 3RQG) and Vinculin (PDB ID: 3H2U) [15,28,35]. In silico mutations were introduced using Python molecular viewer (PMV) [36] without further energy minimization of mutants. HADDOCK webserver with expert access (http://haddock.science.uu.nl/enmr/services/HADDOCK2.2/haddockserver-expert.html) was used for calculating restrained docking solutions [37]. Ambiguous restraints were taken as residues within 4 Å from any atom of the peptide in LDBD. This allowed exploring more interactions on the defined surface. Unambiguous distance restraints (UIRs) were defined for active residues that make conserved interactions. For example, Asp of LD motifs is always observed to interact with Arg or Lys residue in LDBDs. This restraint ensures that the LD peptides dock in the correct orientation and not in an inverted direction. List of residues taken to define ambiguous and Unambiguous distance restraints is given in Supplementary Table S3. Passive residues were defined automatically around active residues. No center of mass restrains and surface contact restraints were given. Default protonation states were taken for all Lys and Arg residues. AIR is an ambiguous distance between a pair of amino acid residues shown to be involved in a particular protein-protein interaction [38].

1000 iterations of rigid-body docking, each with five trials of energy minimization followed by semiflexible and explicit solvent refinements were carried out on top 200 structures with the lowest energy. HADDOCK score is calculated as the weighted sum of van der Waals (E_{vdw}), electrostatic energy (E_{elec}), restraints violation energy (E_{dist}), and desolvation energy (E_{desol}) in kcal/mol [37]. Docking solutions were clustered based on a 2 Å r.m.s.d. cut-off. Each cluster was scored based on the top five structures of the lowest energy set. Images were displayed by PyMOL (The PyMOL Molecular Graphics System, Version 1.5.0.1 Schrödinger, LLC).

2.4. Molecular cloning

The Focal adhesion targeting domain of Chicken Focal adhesion kinase (amino acid: 905–1053) was sub-cloned from a full length construct into a 6His-tag containing modified pET-M vector between BamH1 and Xho1 sites. The following primer sequences were used; forward primer: GCGGATCCATCAAGCCACAGGAAATC, reverse primer: GCCTCGAGTTAGTGGGGCCTGGACTG. Double point mutations were introduced in the wild type construct by site directed mutagenesis using following primer sequences: (N992K, K989V): GGCCCAGGTACTGCTG AAGTCTGACC (forward primer), (N992K, K989 N): GGCCCAGAATCT GCTGAAGTCTGACC (forward primer). The mutated DNA was transformed into *E.coli* XL1-blue cells and plated on antibiotic containing agar plate. The correct in-frame mutations were confirmed by sequencing of selected clones.

2.5. Protein expression and purification

The modified pET32a plasmids were transformed into *E.coli* BL21 (DE3) cells. The cells were grown in LB broth at 37 °C. Once the optical density of the culture was 0.3–0.5, the protein expression was induced

by adding 1 mM IPTG. The cells were harvested by centrifugation and resuspended in 20 mM Tris-HCl (pH 8), 200 mM NaCl, 5 mM DTT, 1% TritonX-100, 5% glycerol and protease inhibitor (Roche). The cells were lysed by sonication of the cell suspension on ice. The lysates were centrifuged and the supernatant was transferred to previously washed Ni-NTA beads for overnight binding. After three washes, the protein was eluted from beads in two elution steps. The elution buffer had 20 mM Tris-HCl (pH 8), 150 mM NaCl, 5% glycerol and 5 mM DTT in addition to 200–300 mM Imidazole. The eluted protein was loaded on pre-equilibrated Superdex75 column for further purification by size exclusion chromatography. The fractions were collected and were stored in 20 mM Tris-HCl (pH 8) and 150 mM NaCl. The homogeneity of the protein was assessed by dynamic light scattering and SDS-PAGE (Supplementary Fig. S5).

2.6. Isothermal titration calorimetry

All ITC titrations were performed on a VP-ITC calorimeter (MicroCal, LLC, Northampton, MA, USA) at 25 °C. The reference cell was filled with the same buffer solution as that used for the protein. Peptides of grade > 98% purity were purchased from GL Biochem (Shanghai) Ltd. and used without further purification. The sequences of the peptides were as follows; LD1: MDDLDALLADLEST, LD2: LSELDRLLLELNAV, LD4: TRELDELMASLSDF. These included the consensus LD motif sequence, as underlined, together with three additional amino acids at both N- and C-terminus. The sample cell of the micro-calorimeter was cleaned thoroughly. 40–50 μM protein, purified by gel filtration in 20 mM Tris (pH 8) and 150 mM NaCl, was placed in the sample cell, and was titrated with 0.9–1 mM peptide solution prepared freshly in identical buffer as that of the protein. The samples were subjected to high speed spin for 5 min and degassed prior to titrations. Heats given by injections, each of 10 μL volume, were recorded at equally spaced intervals of seven minutes. The heat effects per injection were calculated by integration and were normalized by the amount of LD peptide added per injection. All titrations were analyzed with a model considering 'n' identical and independent ligand binding sites implemented in Origin 7.0 (Origin Lab Corp., Northampton, MA, USA) software. There is no need for assuming a model considering non-identical binding sites or cooperative binding sites (with one exception, discussed in results). At least two replicates for each experiment were performed (Supplementary Fig. S2). Statistical parametric (F-test) and non-parametric (Akaike's Information Criterion) tests have been applied in order to compare the statistical performance of binding models, regarding mainly the number of binding-competent binding sites. The results (binding affinity, stoichiometry) shown in Table 3 and Supplementary Table S5 represent the most appropriate results according to these comparison tests.

2.7. Cell culture, transfection and imaging

MCF7 cells were grown in high-glucose DMEM (Hyclone), 10% fetal bovine serum, 100 units/mL penicillin, and 100 μg/mL streptomycin (Hyclone). The cells were grown at 37 °C and 5% CO_2. MCF7 cells were seeded in 6-well plates and were transfected with 1 μg of wild type and mutated FAK plasmids using Mirus (TransIT). 35 mm glass bottom culture dish (Ibidi) were coated with 10 μg/cm^2 of rat tail collagen Type I (Sigma) for 1 h at 37 °C. 10^4 of MCF7 cells were trypsinized and seeded on a glass bottom dish for 5 min and imaged using a spinning disk confocal microscope (PerkinElmer) at 37 °C, 5% CO_2. The images were background subtracted and analyzed with the image analysis software, Imaris (Bitplane). The region of Interest (i.e. focal adhesion) was masked. Autoregressive motion was used to track the changes in the area over the indicated time points. A change in area of at least 95 focal adhesions over a period of 40 mins was quantified for each sample. The values were plotted, and statistical significance of the data was calculated by unpaired *t*-test with Welch's Correction using GraphPad Prism version 6.0c for Mac, GraphPad Software, La Jolla California USA. The Welch's t-test, or unequal variances t-test was used to determine the asymptotic significance of the data as an adaptation of Student's t-test,due to its higher reliability when the two samples have unequal variances and/or unequal sample sizes.

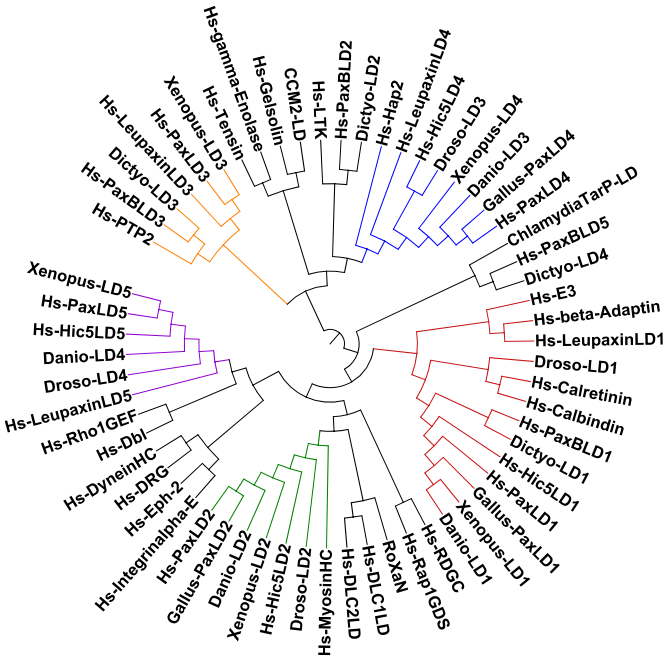

Fig. 1. Phylogenetic tree of LD motifs.
Neighbor-joining tree created using 14-mer LD-peptides taken from Paxillin, PaxB, Hic-5 and Leupaxin sequences of Human, Gallus, Drosophila, Xenopus, Danio, Dictyostellium is shown. The LD motif sequences were also taken from CCM2, Chlamydia, DLC1, DLC2, RoXaN, Gelsolin and from literature [4,10,12,14]. Branches were colored to show various clusters. Five distinct groups corresponding to LD1 (red), LD2 (green), LD3 (orange), LD4 (blue), and LD5 (purple) motifs were clearly differentiated from other unconventional LD motif such as from Chlamydia and proteins other than Paxillin or its homologues. The tree is displayed using iTOL [31].

3. Results

3.1. LD motifs and their conservation across organisms

We first constructed a cladogram using 14-mer LD motif sequences of Paxillin, Hic5, Leupaxin, PaxB and other proteins from the literature [4,10,12,14] (Fig. 1). They were identified from Human, *Xenopus*, *Danio*, *Dictyostelium*, *Gallus* and *Drosophila* genomes to make the dataset more comprehensive. Broadly, the tree showed clustering in five distinct groups named as LD1 to LD5 (taking human Paxillin as reference). Unconventional LD motifs, such as DLC1-LD, do not cluster with any of these groups. On the basis of clustering, we propose that they might exhibit different binding properties with typical LDBDs. Thus, LD motifs also form an important class of protein recognition motifs.

PaxB isoform is closer to slime mold Paxillin sequence. The conventional LD1, LD2, and LD4 motifs are slow evolving as compared to LD3 and LD5. The LD motifs of Calretinin, Calbinding, and β-adaptin, which cluster closely to LD1 motif branch, can be explored for their ability to interact with typical LDBDs that provide grove between helices for LD binding. The LD motif of pathogen Chlamydia was closely related to LD5 motif for which no LDBD has been identified yet. Thus, knowledge of more divergent LDBDs will help to understand host-pathogen relations. Similarly, RoXaN clustered most closely with divergent LD motifs of Deleted in Liver Cancer (DLC) protein, which is known to interact with Talin and FAK [11,13] . Further, the greater

Table 1
Number of hydrophobic and electrostatic interactions within a cut-off distance of 4 Å in structures of FAKFAT, CCM3 and α-parvin with three LD motifs.

Domain peptide pairs	PDB ID	No. of C-C contacts	Average C-C distance (Å)	No. of electrostatic interactions	Residues involved in electrostatic interactions[a]
FAKFAT-LD2[b]	1OW8	16	3.65	7	Arg962, Lys955, Lys1002
FAKFAT-LD4	1OW7	15	3.63	6	Arg962, Lys955, Lys1002
CCM3-LD1	3RQE	16	3.74	3	Lys139,Lys132
CCM3-LD2	3RQF	14	3.81	3	Lys179,Lys172
CCM3-LD4	3RQG	19	3.81	4	Lys179, Lys172,Ser175
α-parvin-LD1	2VZD	22	3.79	6	Arg369,Lys260
α-parvin-LD2	2VZG	17	3.78	4	Arg369
α-parvin-LD4	2VZI	27	3.85	4	Arg369

[a] Only those residues are listed which made electrostatic contacts through their side-chain atoms.
[b] FAT domain of FAK does not bind with LD1.

number of LD motifs in higher species might be related to evolving versatility of such LD motifs.

3.2. LD motif binding domains (LDBDs)

A number of domains are known to bind to LD motifs (Supplementary Table S1), however, no conserved sequence motif is known for LD motif binding. To understand the key determining factors for binding affinity, we first analyzed the available crystal structures of FAKFAT domain in complex with LD motifs [15] and compared them with LD bound complexes of CCM3 [28] and α-parvin [16]. To date, these are the only three dimensional structures available in complex with all three LD motifs (LD1, LD2, LD4) except FAKFAT which is not known to bind with LD1. To assess hydrophobic burial, we counted the number of C-C contacts between any of C-atom of LDBD and that of LD motif within 4 Å using CCP4 suite, and also calculated the average C-C distances [39]. Similarly, the number of electrostatic interactions (defined as any two atoms with opposite partial charges belonging to separate chains within 4 Å) were calculated (Table 1). We found that the number of C-C contacts as well as C-C distances were not significantly different among three structures. The distances range from 3.6 Å to 3.9 Å. The higher number of C-C interactions in α-parvin-LD1 and α-parvin-LD4 (22 and 27 respectively) indicate that hydrophobic burial is the main driving force for their interaction. Further, for a given structure, the number of electrostatic interactions were similar when compared across three LD motifs. Thus, we conclude that neither the number of hydrophobic nor the number of electrostatic interactions determine specificity of three LD motifs towards LDBDs.

On binding surface of LDBDs, a few key residues have been marked to be important for LD binding in earlier studies [15], e.g. Arg/ Lys, which interact via salt bridge interaction with the Asp/ Glu of LD motifs. A closer look of the binding surface of FAKFAT (PDB ID: 1OW6), CCM3 (PDB ID: 3RQG) and Vinculin tail domain (PDB ID: 3H2U) revealed that such interacting Arg/ Lys residues were present in unique arrangement at four positions on these LDBDs. These positions were named as pos1-pos4 (Table 2, Supplementary Fig. S6). In FAKFAT (PDBID: 1OW7), these positions are occupied by R962 (pos1), K955 (pos2), K1002 (pos3), K988 (pos4) residues. The distances between the Cα atoms of these residues were same in all three LDBDs, e.g. pos1 and pos2 were separated by ~10 Å distance and two helical turns. Only the Lys residue at pos4 was present at variable distances in three structures, i.e. two, three and four helical turns apart from pos3 in CCM3, FAK and Vinculin LDBDs respectively (Table 2). Thus, we created various mutants by changing the position of Lysine at pos4 in all three structures to mimic the LD binding surface of FAK, Vinculin and CCM3 LDBDs, in order to analyze the effect of relative position of Lysine on binding affinity. Since LD4 motif specifically binds only between helix2 and helix3 of FAKFAT [32], we did not mutate other LD binding site between helix1 and helix4 known in FAKFAT. Further, the geometrical features observed for site between helix1 and helix4, were not comparable to common features observed for FAT (helix2-helix3 site), CCM3 and Vinculin (Fig. 2, Supplementary Fig. S6).

Table 2
Geometric features between residues at pos^{3} and pos^{4} for various LDBDs.

LDBDs	[a]Distance (Å)	[a]Number of turns
FAKFAT	21.3	4
Vinculin tail	17.5	3
CCM3	10.7	2

[a] The corresponding positions are pos^{4-1} and pos^{4-2} for Vinculin tail and CCM3 respectively.

3.3. LD-FAKFAT docking analysis

We created *in-silico* mutants of FAKFAT (PDB ID: 1OW6), CCM3 (PDB ID: 3RQG), and Vinculin tail (PDB ID: 3H2U) domains by residue swapping. For example, the Lys at pos4 (K988) in FAKFAT was swapped with residue at one helical turn (N991) and two helical turns (G995) so as to match the geometrical arrangements observed in Vinculin tail and CCM3 LDBDs respectively. These were named as FAT(V-like) and FAT(C-like) arrangements. The FAT(F-like) geometry refers to the arrangement of residues found in wild type FAKFAT domain. In Vinculin tail, the poorly defined LD motif binding surface is masked by a largely hydrophobic N-terminal helix. This helix was deleted to expose the LD motif binding surface for docking experiment. Similarly, Vinculin(C-like) and Vinculin(F-like) mutants were created by swapping K924 with L928, and A921 respectively in Vinculin tail domain. For CCM3, K172 was moved one helical turn to swap with V168 so as to match geometrical arrangement observed in Vinculin tail (CCM3(V-like) mutant). The CCM3(F-like) arrangement was same as wild type CCM3, as it has Lysine at both positions. Residues restraints were given to explore docking on desired binding surfaces. For example, FAKFAT has two binding sites and LD1 binds CCM3 in opposite orientation as compared to LD2 and LD4. Restraints restricted binding to a given site of FAKFAT and known orientation of LD1 in CCM3. The values were compared with their known lowest affinity LDBD. The C-like conformations in all three LDBDs showed increased buried surface area and lower electrostatic energy. Based on this we concluded that changing the position of Lysine improved the binding of LD motifs with their known lowest affinity LDBD (Supplementary Table 4).

3.4. Isothermal titration calorimetry

Homogenous fractions of purified wild type and mutant *Gallus* FAKFAT domains were titrated with three LD motifs. *Gallus* FAKFAT has A996 at $pos4^{-2}$ instead of G995 of human FAKFAT (analyzed in docking). We first created two C-like mutants named as FAT(AKKV) and FAT(A996K). Similar to CCM3, FAT(A996K) mutant had Lysine at both $pos4^{-2}$ and pos4. FAT(AKKV) was a double mutant (A996K and K989V) in which Alanine was replaced by Lysine two helical turns above to match CCM3 configuration. The Lysine at pos4 was replaced

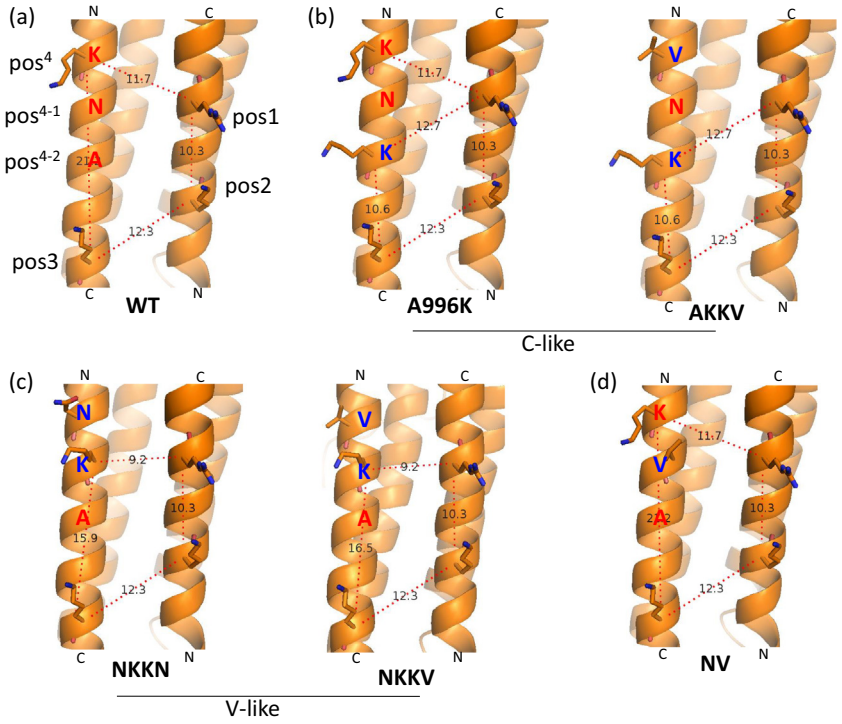

Fig. 2. FAKFAT mutants.
Four positions found to be critical for binding with LD motif are shown on Focal adhesion targeting domain of Human Focal Adhesion Kinase (FAKFAT). They are occupied by Arg962 (pos1), Lys955 (pos2), Lys1002 (pos3) and Lys988 (pos4) residues in Gallus FAKFAT. Pos3 and pos4 are separated by four helical turns in FAKFAT domain. The wild type residues are shown in red and mutated ones in blue. (b) The Lys988 residues was moved to pos4^{-2} to match geometric arrangement as seen in CCM3, thus named C-like mutants. (c) The other pair of mutant is named V-like where Lys988 was moved one helical turn towards pos3. (d) Only Asn992 was mutated with Valine while conserving the positions of Lysines. Thus, the geometrical arrangement is similar to wild type. The mutant is named as FAT(NV).

by Valine to make it hydrophobic without major compromise in side chain length (Fig. 2). In another set of mutants named as FAT(NKKV) and FAT(NKKN), the configuration was matched to Vinculin tail. In FAT(NKKV) mutant, N992 at pos4^{-1} was replaced by Lysine and Lysine at pos4 was replaced with Valine while in FAT(NKKN) mutant, Lysine and Asparagine residues at pos4 and pos4^{-1} were swapped so as to maintain the overall charge at the binding surface.

In our experiments, the wild type domain could interact with LD2 and LD4 with 63 μM and 71 μM dissociation constants, respectively, and two binding sites were observed as expected. The values observed are different as compared to earlier studies because of different experimental conditions and different length of peptide used. LD1 motif does not bind to wild type domain (Fig. 3, Table 3). For both FAT(A996K) and FAT(AKKV) mutants LD1 exhibited very low affinity ($K_d \geq 500$ and 400 μM respectively) (Supplementary Fig. S1 and Supplementary Table S5). LD2 and LD4 could interact with these mutants with comparable affinity as wild type, however, the stoichiometry of binding changed from two binding sites to one binding site. LD4, showed a slight improvement in binding affinity to A996K mutant (K_d = 58 μM) as compared to wild type (Supplementary Table 5). The result indicated that the binding surface near pos4 affects the binding affinity for three LD peptides, but the differences were not found to be very large.

The V-like mutants, i.e. FAT(NKKN) and FAT(NKKV), showed remarkable improvement in K_d values. The stoichiometry of binding also changed to one in both the mutants and with all three peptides. LD2 and LD4 showed five-fold and seven-fold stronger binding to swap mutant FAT(NKKN) as compared to wild type. LD1 could bind with 48 μM dissociation constants as compared to no binding with wild type domain. The binding was even stronger when Lysine at pos4 is mutated to hydrophobic residue Valine (FAT(NKKV) mutant) with K_d value of 9.1 μM for LD1. LD2 peptide binds 2.4 times stronger, while a small change in K_d value was observed for LD4 interacting with FAT(NKKV) mutant. This indicates that LD1 significantly preferred FAT(NKKV) mutant, while FAT(NKKN) mutant was favored for binding of LD2 and LD4. The results strongly indicated that residues at pos4 of binding surface in LDBD are key factors modulating and controlling the binding affinities of LD peptides with LDBDs. Further, to test the preference for a hydrophobic residue at pos4, we mutated N992 at pos4^{-1} to V, while keeping Lys at pos4 unchanged (named as FAT(NV) mutant). Notably, the dissociation constant of LD1 peptide with FAT(NV) mutant was 1.5 μM as compared to no binding with the wild type FAT domain. LD2-peptide showed nine-fold stronger binding (7.2 μM), while LD4 did not interact with FAT(NV) mutant. We conclude that LD1 peptide prefers a hydrophobic residue at pos4 or pos4^{-1}. Our mutants are especially important since LD1 is unknown to bind FAT domain of FAK and we could identify a single point mutant FAT(NV) with high affinity (Figs. 2, 3).

In all interactions tested, except in the case of FAT(NV) with LD2, there was no need for considering two non-identical binding sites or cooperative binding sites; the model considering a single set of identical and independent binding sites (with n = 1 or n = 2) was sufficient for reproducing the experimental data. In fact, imposing two different binding sites (with different binding affinity) or imposing a single binding site in some cases (e.g., FAT(WT) titrated with LD2 and LD4) resulted in either no convergence or dependence between fitting parameters (when considering two different binding sites) or a remarkably poor fitting (much larger chi-square). One of the assays for FAT(NV) interacting with LD2 could be fitted either by considering a single binding site and a concentration dependent background injection heat or considering two different binding sites. The first case is the most appropriate, according to a non-parametric model comparison statistical test (Akaike's Information Criterion) (results shown in Table 3), whereas in the second case the first site would exhibit two-fold higher affinity than that reported in Table 3, and the second binding site would have approximately ten-fold lower binding affinity. Both cases however, are suggestive of stronger affinity with FAT(NV). The other replicate of FAT(NV) interacting with LD2 shown in Supplementary Information clearly indicates the presence of a single binding site (Supplementary Fig. S2).

3.5. Cell based experiments

Next, we sought to understand the physiological relevance of the wild-type and high affinity mutants of the FAT domain of FAK. We examined the turnover rate of focal adhesions of MCF7 cells expressing the GFP-tagged wild type, FAK(NV), FAK(NKKV) and FAK(NKKN)

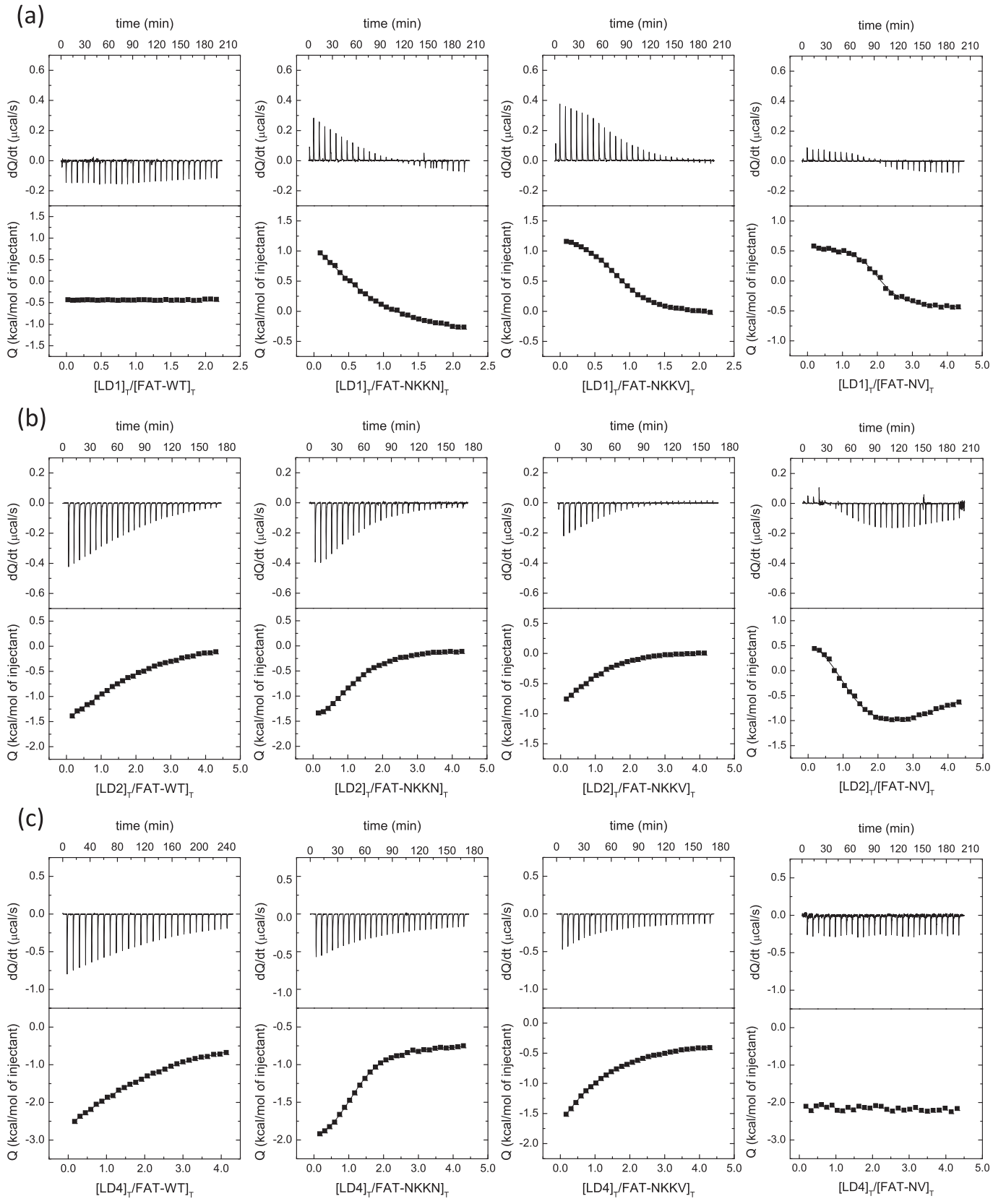

Fig. 3. Isothermal titration calorimetry experiments of FAT(NKKV), FAT(NKKN) and FAT(NV) mutants interacting with LD1, LD2 and LD4 motifs.
Isothermal titration calorimetry curves (thermograms, upper plots; binding isotherms, lower plots) are shown for wild type and high affinity mutants of FAKFAT. This includes V-like mutants (FAT(NKKN) and FAT(NKKV)) and FAT(NV) mutants interacting with (a) LD1 (b) LD2, and (c) LD4. Closed squares represent the experimental data and continuous lines represent the non-linear least squares fitting curves.

Table 3
Thermodynamics of binding between LD motifs and high affinity mutants of FAKFAT domain.

LD motif	FAKFAT domain	K_d (μM)	ΔG (kcal/mol)	ΔH (kcal/mol)	-TΔS (kcal/mol)	n
LD1	WT	–	–	–	–	–
	NKKN	48 ± 13	−5.9 ± 0.2	2.5 ± 0.5	−8.4 ± 0.5	0.8 ± 0.1
	NKKV	9.1 ± 0.9	−6.9 ± 0.1	1.4 ± 0.4	−8.3 ± 0.4	0.9 ± 0.1
	NV	**1.5 ± 0.3**	**−7.9 ± 0.1**	**1.0 ± 0.3**	**−8.9 ± 0.3**	**2.0 ± 0.1**
LD2	WT	63 ± 14	−5.7 ± 0.1	−2.7 ± 0.5	−3.0 ± 0.5	1.8 ± 0.1
	NKKN	16 ± 4	−6.5 ± 0.2	−1.7 ± 0.4	−4.8 ± 0.4	1.2 ± 0.1
	NKKV	26 ± 7	−6.3 ± 0.2	−1.3 ± 0.4	−5.0 ± 0.4	1.0 ± ±
	NV	**7.2 ± 0.9**	**−7.0 ± 0.1**	**3.3 ± 0.3**	**−10.3 ± 0.3**	**1.2 ± 0.1**
LD4	WT	71 ± 15	−5.7 ± 0.1	−4.8 ± 0.4	−0.9 ± 0.4	1.9 ± 0.1
	NKKN	**10 ± 2**	**−6.8 ± 0.1**	**−1.4 ± 0.3**	**−5.4 ± 0.3**	**1.2 ± 0.1**
	NKKV	67 ± 16	−5.7 ± 0.1	−3.5 ± 0.4	−2.2 ± 0.4	0.9 ± 0.1
	NV	–	–	–	–	–

The mutant exhibiting strongest binding is shown in bold.
Statistical parametric (F-test) and non-parametric (Akaike's Information Criterion) tests have been applied in order to compare the statistical performance of binding models, regarding mainly the number of binding-competent binding sites. The results (binding affinity, stoichiometry) shown in this table represent the most appropriate results according to these comparison tests.

mutants (Fig. 4). The wild type showed an average turnover of 1.5×10^{-3} μm²/s. Intriguingly, stable focal adhesions were observed in cells expressing the FAK(NV) mutant, which has the slowest turnover rate of 2.5×10^{-5} μm²/s, while the cells expressing FAK(NKKV) have the highest turnover of 3.5×10^{-3} μm²/s. The cells expressing FAK (NKKN) mutant have a focal adhesion turnover rate at 4.5×10^{-4} μm²/s. This finding suggests that the focal adhesion of cells expressing FAK (NV) mutant are stable, while the focal adhesion of cells expressing FAK (NKKV) mutant are more dynamic similar to those in wild type. Consistent with ITC results, the remarkable higher affinity of FAK(NV) mutant with Paxillin LD motifs resulted in high stability of the focal adhesions.

4. Discussion

The regulated interaction of FAK and Paxillin at focal adhesions is required for collective cell migration via down regulating Rac1 activity [40,41], formation and maintenance of cadherin-based cell junctions in migrating cells [42] and also for gene transcription [43]. Elevated expression of FAK is related to brain astrocytomas [44–46] and many diseases [47]. FAK and Paxillin have been widely reviewed for their potential as drug targets for treatment of various cancers [48–51] which further emphasize the importance of studying their interaction.

By varying the relative position of single Lysine residues, nature has wisely chosen to optimize the strength of protein-protein interactions and thus downstream signaling. As shown in this study, moving Lysine one helical turn in FAT(NKKV) mutant improved the binding affinity while moving two helical turns (C-like mutants) did not make significant differences. This showed that the Vinculin-like spatial arrangement of the four residues is the most favorable arrangement. In addition, the complementarity of charged surfaces and hydrophobic interaction is a critical factor governing the affinity of these interactions. This complementarity of charged surface can differentiate various LD motifs although the key binding residues remains the same. Both LD2 and LD4 preferred FAT(NKKN) mutation over FAT(NKKV) due to better complementarity of the charged surfaces. The FAT(NKKN) mutant suggested that even when Lysine residue is available for bonding with Glu of LD4, the presence of another positively charged residue is important, although the position of Lysine residue and Asparagine residues were interchangeable.

The complementarity of charged surface is exemplified by CCM3 also where the loss of interactions at pos4 lead to the tilted binding conformation and thus reduced affinity for LD4. The relatively strong binding of LD4 motif between helix2/helix3 of FAKFAT might be due to optimal inter helical distance as compared to between helix1/helix4 interface and thus providing better complementarity. The positions of Lysine residues are also relatively different and binding is additionally satisfied via the contacts between Glu of LD4 with Lys and Asn (pos4), Ser of LD4 with Lys (pos2), Thr of LD4 with Lys (pos1), and Ser with Lys (pos3). LD2 binding at helix1/helix4 is satisfied by the interaction of Histidine with Asn at the C-terminus of LD2 motif (distance 3.9 Å). Similarly, the higher inter-helical distance in CCM3 as compared to FAKFAT could have caused the reduced binding affinity of LD4 with CCM3 and tilted binding conformation. The additional electrostatic interactions similar to FAKFAT are missing in CCM3, thus resulting in a weaker affinity for LD4. Such interactions resulting in better charge complementarity are important factors for determining the binding affinity and specificity. The optimal conformation also results in better complementarity of hydrophobic surfaces and thus burial of hydrophobic residues of LD motif in the helical grove of FAKFAT domain. By facilitating the improvement in complementarity, notably, a single point mutation FAT(NV) is identified in this study that enabled LD1 peptide to bind to FAKFAT domain with very high affinity leading to > 100 times stable focal adhesions.

LD2 and LD4 motifs can bind on two binding surfaces on FAKFAT at the same time and presence of both binding sites on FAK can give 5–10 fold higher affinity with Paxillin [32,52]. In our experiment, LD1 binds with high affinity to FAT(NV) in 2:1 ratio. We discuss that the LD1 binding to FAK(NV) mutant could have induced the sequential binding of Paxillin LD motifs on two FAK(NV) surfaces, similar to simultaneous binding of LD2 and LD4 motifs with wild type, although with much higher binding affinity. Thus, the focal adhesions are highly stable in MCF7 cells expressing FAT(NV) mutant. FAK(NKKN) mutant has higher focal adhesion turnover rate compared to FAK(NV) mutant but lower than wild type. This is explained by the fact that FAK(NKKN) mutant exhibited higher affinities with three peptides (K_d = 48, 16, 10 respectively) but with stoichiometry of 1 (Table 1). FAK(NKKV) shows enhanced binding to LD1 and LD2 motifs with only 1:1 ratio (Table 3), thus exhibits even higher turnover rate as that of the wild type which exhibits two site binding. This suggests that sequential binding on two sites of FAKFAT, induced by FAT(NV) mutation, is also critical for determining overall focal adhesion turnover rate.

Supplementary data to this article can be found online at https://doi.org/10.1016/j.bbagen.2019.129450.

Author contribution

ABG conceived the idea, planned the study, did bioinformatics

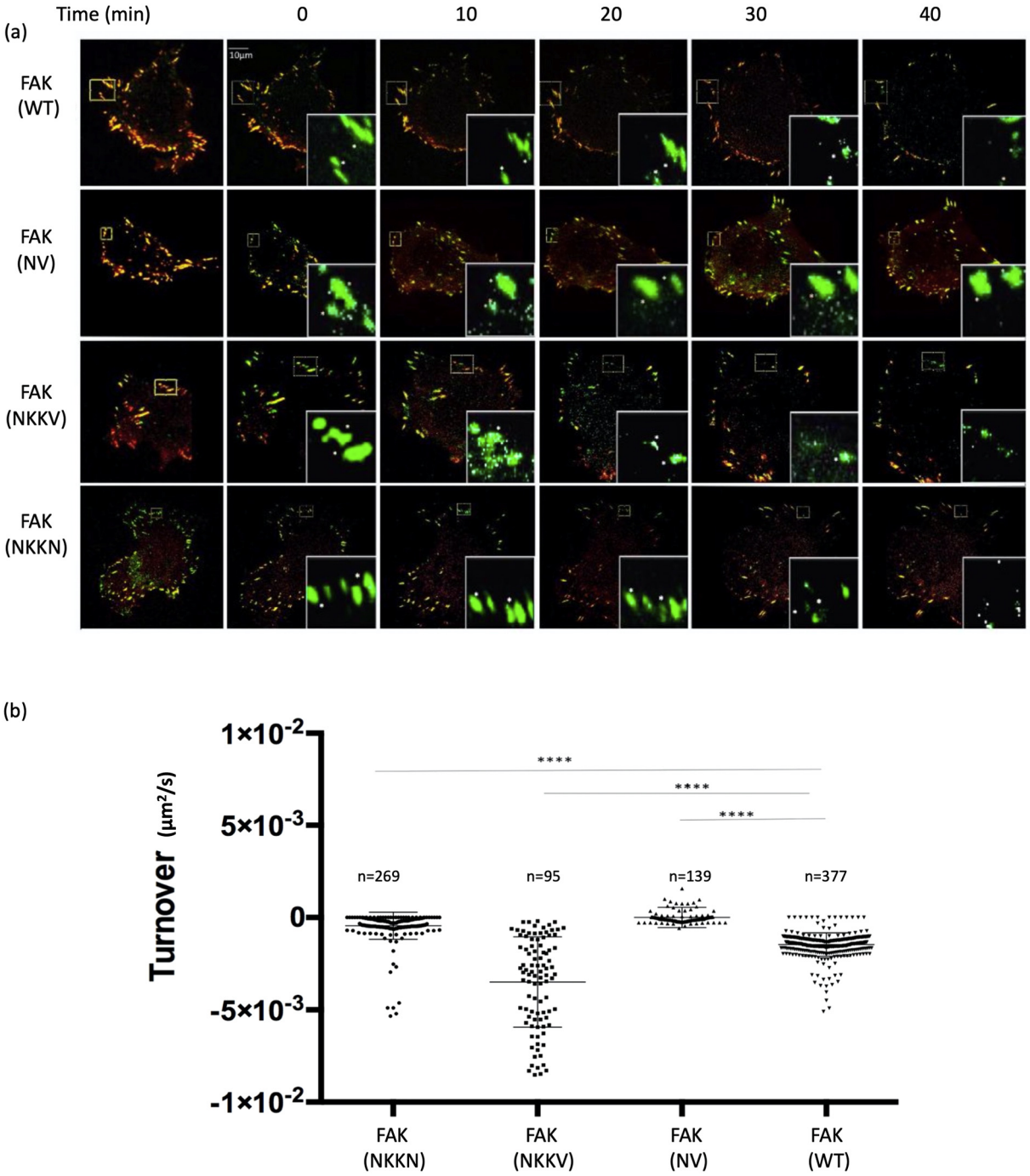

Fig. 4. Focal adhesion turnover of different FAK mutants in cell based assay.
(a) Time-lapse of the focal adhesion of MCF7 cells transfected with mApple-tagged paxillin and the various GFP-tagged wildtype or mutants of FAK were imaged using confocal microscope. The focal adhesion turnover was measured and quantified over a period of 40 mins. (b) Graphical representation of the change in focal adhesion area ($\mu m^2/s$) of the MCF7 cell co-expressing GFP-tagged wild type or mutants of FAK and mApple-tagged paxillin over a period of 40 mins.

analysis and ITC experiments, analyzed results and wrote the manuscript. BCL supervised the study. BCL and JS critically reviewed results and the manuscript. SM and CPQ did experiments related to cell lines and analyzed the data. AVC analyzed ITC data and critically reviewed the manuscript.

Declaration of Competing Interest

Authors declare no conflict of interests associated with this manuscript.

Acknowledgements

This work was supported by the Mechanobiology Institute Singapore and by the Singapore Ministry of Education Academic Research Fund Tier 3 (MOE Grant No: MOE2016-T3-1-002) to B.C.L. J.S was supported by AcRF Tier-1 grant (R154-000-A72-114).

References

[1] M.D. Schaller, Paxillin: a focal adhesion-associated adaptor protein, Oncogene 20 (2001) 6459–6472.

[2] M.C. Brown, C.E. Turner, Paxillin: adapting to change, Physiol. Rev. 84 (2004) 1315–1339.
[3] D.A. Tumbarello, M.C. Brown, C.E. Turner, The paxillin LD motifs, FEBS Lett. 513 (2002) 114–118.
[4] M.C. Brown, M.S. Curtis, C.E. Turner, Paxillin LD motifs may define a new family of protein recognition domains, Nat. Struct. Mol. Biol. 5 (1998) 677–678.
[5] M.E. Manetti, S. Geden, M. Bott, N. Sparrow, S. Lambert, C. Fernandez-Valle, Stability of the tumor suppressor merlin depends on its ability to bind paxillin LD3 and associate with β1 integrin and actin at the plasma membrane, Biol. Open 1 (2012) 949–957.
[6] N. Nishiya, T. Shirai, W. Suzuki, K. Nose, Hic-5 interacts with GIT1 with a different binding mode from Paxillin, J. Biochem. 132 (2002) 279–289.
[7] C.E. Turner, Paxillin interactions, J. Cell Sci. 113 (2000) 4139.
[8] S. Kaushik, A. Ravi, F.M. Hameed, B.C. Low, Concerted modulation of paxillin dynamics at focal adhesions by deleted in liver cancer-1 and focal adhesion kinase during early cell spreading, Cytoskeleton 71 (2014) 677–694.
[9] T. Alam, M. Alazmi, R. Naser, F. Huser, A.A. Momin, K.W. Walkiewicz, C.G. Canlas, R.G. Huser, A. Ali, J. Merzaban, V.B. Bajic, X. Gao, S.T. Arold, Proteome-level Assessment of Origin, Prevalence and Function of LEUCINE-Aspartic Acid (LD) Motifs, (2018), p. 278903.
[10] K.M. Draheim, X. Li, R. Zhang, O.S. Fisher, G. Villari, T.J. Boggon, D.A. Calderwood, CCM2–CCM3 interaction stabilizes their protein expression and permits endothelial network formation, J. Cell Biol. 208 (2015) 987–1001.
[11] G. Li, X. Du, W.C. Vass, A.G. Papageorge, D.R. Lowy, X. Qian, Full activity of the deleted in liver cancer 1 (DLC1) tumor suppressor depends on an LD-like motif that binds Talin and focal adhesion kinase (FAK), Proc. Natl. Acad. Sci. 108 (2011) 17129–17134.
[12] T.R. Thwaites, A.T. Nogueira, I. Campeotto, A.P. Silva, S.S. Grieshaber, R.A. Carabeo, The chlamydia effector TarP mimics the mammalian LD motif of Paxillin to subvert the focal adhesion kinase during invasion, J. Biol. Chem. 289 (44) (2014) 30426–30442.
[13] T. Zacharchenko, X. Qian, Benjamin T. Goult, D. Jethwa, Teresa B. Almeida, C. Ballestrem, David R. Critchley, Douglas R. Lowy, Igor L. Barsukov, LD motif recognition by talin: structure of the talin-DLC1 complex, Structure 24 (7) (2016) 1130–1141.
[14] T. Alam, M. Alazmi, X. Gao, S.T. Arold, How to find a leucine in a haystack? Structure, ligand recognition and regulation of leucine–aspartic acid (LD) motifs, Biochem. J. 460 (2014) 317–329.
[15] M.K. Hoellerer, M.E.M. Noble, G. Labesse, I.D. Campbell, J.M. Werner, S.T. Arold, Molecular recognition of paxillin LD motifs by the focal adhesion targeting domain, Structure 11 (2003) 1207–1217.
[16] S. Lorenz, I. Vakonakis, E.D. Lowe, I.D. Campbell, M.E.M. Noble, M.K. Hoellerer, Structural analysis of the interactions between paxillin LD motifs and α-parvin, Structure 16 (2008) 1521–1531.
[17] X. Tong, P.M. Howley, The bovine papillomavirus E6 oncoprotein interacts with paxillin and disrupts the actin cytoskeleton, Proc. Natl. Acad. Sci. U. S. A. 94 (1997) 4412–4417.
[18] G. Gao, K.C. Prutzman, M.L. King, D.M. Scheswohl, E.F. DeRose, R.E. London, M.D. Schaller, S.L. Campbell, NMR solution structure of the focal adhesion targeting domain of focal adhesion kinase in complex with a paxillin LD peptide, J. Biol. Chem. 279 (2004) 8441–8451.
[19] Z.M. Zhang, J.A. Simmerman, C.D. Guibao, J.J. Zheng, GIT1 paxillin-binding domain is a four-helix bundle, and it binds to both paxillin LD2 and LD4 motifs, J. Biol. Chem. 283 (2008) 18685–18693.
[20] M.S. Vanarotti, D.J. Miller, C.D. Guibao, A. Nourse, J.J. Zheng, Structural and mechanistic insights into the interaction between Pyk2 and paxillin LD motifs, J. Mol. Biol. 426 (2014) 3985–4001.
[21] J. Lulo, S. Yuzawa, J. Schlessinger, Crystal structures of free and ligand-bound focal adhesion targeting domain of Pyk2, Biochem. Biophys. Res. Commun. 383 (2009) 347–352.
[22] Paxillin: a new vinculin-binding protein present in focal adhesions, J. Cell Biol. 111 (1990) 1059–1068.
[23] C. Bakolitsa, J.M. de Pereda, C.R. Bagshaw, D.R. Critchley, R.C. Liddington, Crystal structure of the vinculin tail suggests a pathway for activation, Cell 99 (1999) 603–613.
[24] M.C. Brown, J.A. Perrotta, C.E. Turner, Identification of LIM3 as the principal determinant of paxillin focal adhesion localization and characterization of a novel motif on paxillin directing vinculin and focal adhesion kinase binding, J. Cell Biol. 135 (1996) 1109.
[25] A.L. Stiegler, K.M. Draheim, X. Li, N.E. Chayen, D.A. Calderwood, T.J. Boggon, Structural basis for Paxillin binding and focal adhesion targeting of β-Parvin, J. Biol. Chem. 287 (2012) 32566–32577.
[26] S. Liu, W.B. Kiosses, D.M. Rose, M. Slepak, R. Salgia, J.D. Griffin, C.E. Turner, M.A. Schwartz, M.H. Ginsberg, A fragment of Paxillin binds the α4Integrin cytoplasmic domain (tail) and selectively inhibits α4-mediated cell migration, J. Biol. Chem. 277 (2002) 20887–20894.
[27] R.T. Böttcher, M. Veelders, P. Rombaut, J. Faix, M. Theodosiou, T.E. Stradal, K. Rottner, R. Zent, F. Herzog, R. Fässler, Kindlin-2 recruits paxillin and Arp2/3 to promote membrane protrusions during initial cell spreading, J. Cell Biol. 216 (2017) 3785.
[28] X. Li, W. Ji, R. Zhang, E. Folta-Stogniew, W. Min, T.J. Boggon, Molecular recognition of leucine-aspartate repeat (LD) motifs by the focal adhesion targeting homology domain of cerebral cavernous malformation 3 (CCM3), J. Biol. Chem. 286 (2011) 26138–26147.
[29] F. Jeanmougin, J.D. Thompson, M. Gouy, D.G. Higgins, T.J. Gibson, Multiple sequence alignment with clustal X, Trends Biochem. Sci. 23 (1998) 403–405.
[30] N. Saitou, M. Nei, The neighbor-joining method: a new method for reconstructing phylogenetic trees, Mol. Biol. Evol. 4 (1987) 406–425.
[31] I. Letunic, P. Bork, Interactive tree of life (iTOL) v3: an online tool for the display and annotation of phylogenetic and other trees, Nucleic Acids Res. 44 (2016) W242–W245.
[32] C.M. Bertolucci, C.D. Guibao, J. Zheng, Structural features of the focal adhesion kinase–paxillin complex give insight into the dynamics of focal adhesion assembly, Protein Sci. 14 (2005) 644–652.
[33] www.rcsb.org/, (2019).
[34] Lee J.H.; Rangarajan E.S.; Yogesha S.D.; Izard T.; Raver1 interactions with vinculin and RNA suggest a feed-forward pathway in directing mRNA to focal adhesions. Structure. 17. 833-842
[35] J.H. Lee, E.S. Rangarajan, S.D. Yogesha, T. Izard, Raver1 interactions with vinculin and RNA suggest a feed-forward pathway in directing mRNA to focal adhesions, Structure (London, England : 1993) 17 (2009) 833–842.
[36] The PyMOL Molecular Graphics System, Version 1.7, LLC:Schrödinger
[37] S.J. de Vries, M. van Dijk, A.M.J.J. Bonvin, The HADDOCK web server for data-driven biomolecular docking, Nat. Protoc. 5 (2010) 883–897.
[38] C. Dominguez, R. Boelens, A.M.J.J. Bonvin, HADDOCK: a protein − protein docking approach based on biochemical or biophysical information, J. Am. Chem. Soc. 125 (2003) 1731–1737.
[39] M.D. Winn, C.C. Ballard, K.D. Cowtan, E.J. Dodson, P. Emsley, P.R. Evans, R.M. Keegan, E.B. Krissinel, A.G.W. Leslie, A. McCoy, S.J. McNicholas, G.N. Murshudov, N.S. Pannu, E.A. Potterton, H.R. Powell, R.J. Read, A. Vagin, K.S. Wilson, Overview of the CCP4 suite and current developments, Acta Crystallogr. D Biol. Crystallogr. 67 (2011) 235–242.
[40] T.B. Deramaudt, D. Dujardin, F. Noulet, S. Martin, R. Vauchelles, K. Takeda, P. Rondé, Altering FAK-Paxillin interactions reduces adhesion, migration and invasion processes, PLoS One 9 (2014) e92059.
[41] A.M. López-Colomé, I. Lee-Rivera, R. Benavides-Hidalgo, E. López, Paxillin: a crossroad in pathological cell migration, J. Hematol. Oncol. 10 (2017) 50.
[42] H. Yano, Y. Mazaki, K. Kurokawa, S.K. Hanks, M. Matsuda, H. Sabe, Roles played by a subset of integrin signaling molecules in cadherin-based cell–cell adhesion, J. Cell Biol. 166 (2004) 283–295.
[43] A.R. Sathe, G.V. Shivashankar, M.P. Sheetz, Nuclear transport of paxillin depends on focal adhesion dynamics and FAT domains, J. Cell Sci. 129 (10) (2016) 1981–1988.
[44] A. Gutenberg, W. Brück, M. Buchfelder, H.C. Ludwig, Expression of tyrosine kinases FAK and Pyk2 in 331 human astrocytomas, Acta Neuropathol. 108 (2004) 224–230.
[45] Z. Li, X. Yuan, Z. Wu, Z. Guo, P. Jiang, Z. Wen, Expressions of FAK and Pyk2 in human astrocytic tumors and their relationship with angiogenesis, Chin.-Ger. J. Clin. Oncol. 7 (2008) 658–660.
[46] T.P. Hecker, J.R. Grammer, G.Y. Gillespie, J. Stewart, C.L. Gladson, Focal adhesion kinase enhances signaling through the Shc/extracellular signal-regulated kinase pathway in anaplastic astrocytoma tumor biopsy samples, Cancer Res. 62 (2002) 2699–2707.
[47] P.P. Eleniste, A. Bruzzaniti, Focal adhesion kinases in adhesion structures and disease, J. Signal Transduct. 2012 (2012) 12.
[48] G.W. McLean, N.O. Carragher, E. Avizienyte, J. Evans, V.G. Brunton, M.C. Frame, The role of focal-adhesion kinase in cancer [mdash] a new therapeutic opportunity, Nat. Rev. Cancer 5 (2005) 505–515.
[49] R. Kanteti, S.K. Batra, F.E. Lennon, R. Salgia, FAK and Paxillin, Two Potential Targets in Pancreatic Cancer, (2016).
[50] G.W. McLean, N.O. Carragher, E. Avizienyte, J. Evans, V.G. Brunton, M.C. Frame, The Role of Focal-Adhesion Kinase in Cancer — a New Therapeutic Opportunity, vol. 5, (2005), p. 505.
[51] M. Nocula-Lugowska, M. Lugowski, R. Salgia, A.A. Kossiakoff, Engineering synthetic antibody inhibitors specific for LD2 or LD4 motifs of paxillin, J. Mol. Biol. 427 (2015) 2532–2547.
[52] J.W. Thomas, M.A. Cooley, J.M. Broome, R. Salgia, J.D. Griffin, C.R. Lombardo, M.D. Schaller, The role of focal adhesion kinase binding in the regulation of tyrosine phosphorylation of Paxillin, J. Biol. Chem. 274 (1999) 36684–36692.